Available online at www.sciencedirect.com
SCIENCE DIRECT
Regulatory Toxicology and Pharmacology 45 (2006) 44–54
Regulatory Toxicology and Pharmacology
www.elsevier.com/locate/yrtph

Revised assessment of cancer risk to dichloromethane: Part I Bayesian PBPK and dose–response modeling in mice

Dale J. Marino [a,*], Harvey J. Clewell [b], P. Robinan Gentry [c], Tammie R. Covington [c], C. Eric Hack [d], Raymond M. David [a], David A. Morgott [a]

[a] *Health, Safety and Environment, Eastman Kodak Company, Rochester, NY 14652, USA*
[b] *CIIT Centers for Health Research, Research Triangle Park, NC 27709, USA*
[c] *ENVIRON Health Sciences Institute, Ruston, LA 71270, USA*
[d] *Toxicology Excellence for Risk Assessment, Cincinnati, OH 45211, USA*

Received 21 September 2005
Available online 25 January 2006

Abstract

The current USEPA cancer risk assessment for dichloromethane (DCM) is based on deterministic physiologically based pharmacokinetic (PBPK) modeling involving comparative metabolism of DCM by the GST pathway in the lung and liver of humans and mice. Recent advances in PBPK modeling include probabilistic methods and, in particular, Bayesian inference to quantitatively address variability and uncertainty separately. Although Bayesian analysis of human PBPK models has been published, no such efforts have been reported specifically addressing the mouse, apart from results included in the OSHA final rule on DCM. Certain aspects of the OSHA model, however, are not consistent with current approaches or with the USEPA's current DCM cancer risk assessment. Therefore, Bayesian analysis of the mouse PBPK model and dose–response modeling was undertaken to support development of an improved cancer risk assessment for DCM. A hierarchical population model was developed and prior parameter distributions were selected to reflect parameter values that were considered the most appropriate and best available. Bayesian modeling was conducted using MCSim, a publicly available software program for Markov Chain Monte Carlo analysis. Mean posterior values from the calibrated model were used to develop internal dose metrics, i.e., mg DCM metabolized by the GST pathway/L tissue/day in the lung and liver using exposure concentrations and results from the NTP mouse bioassay, consistent with the approach used by the USEPA for its current DCM cancer risk assessment. Internal dose metrics were 3- to 4-fold higher than those that support the current USEPA IRIS assessment. A decrease of similar magnitude was also noted in dose–response modeling results. These results show that the Bayesian PBPK model in the mouse provides an improved basis for a cancer risk assessment of DCM.

Keywords: Bayesian modeling; PBPK modeling; Dose–response modeling

1. Introduction

Dichloromethane (DCM, methylene chloride) finds use in industrial processes as an extraction solvent for decaffeinating coffee and as a carrier solvent in the textile and pharmaceutical industries. It also is used in paint strippers and for degreasing of metal parts, and it is well suited for cellulose acetate production (Holbrook, 1993). Prior to the mid-1980s, the primary concern regarding exposure to DCM was oxidative metabolism leading to carboxyhemoglobin formation. Additional studies identified a second metabolic pathway for DCM catalyzed by glutathione transferases (Ahmed and Anders, 1978). Based on these findings, along with experimental evidence that other halogenated hydrocarbons exhibited carcinogenic activity in rodents, several chronic toxicity/oncogenicity studies were initiated in the late 1970s to address questions regarding potential long-term health effects from exposure to DCM (Burek et al., 1984; National Coffee Association, 1982,

* Corresponding author. Fax: +1 585 477 2863.
E-mail address: dale.marino@kodak.com (D.J. Marino).

0273-2300/$ - see front matter © 2005 Elsevier Inc. All rights reserved.
doi:10.1016/j.yrtph.2005.12.007

1983; NTP, 1986; Nitschke et al., 1988; Serota et al., 1986a,b). Results from these studies indicated that inhalation and possibly oral exposures to DCM were associated with carcinogenic activity in mice. A statistically significant increase in hepatocellular adenomas and carcinomas was observed in male B6C3F$_1$ mice following exposure to DCM in drinking water at 50 and 250 mg/kg/day compared to controls, although no dose response was evident (Serota et al., 1986a,b). In addition, treatment-related lung (alveolar/bronchiolar adenomas) and liver (hepatocellular adenomas/carcinomas) tumors were observed in B6C3F$_1$ male and female mice exposed to airborne concentrations of 2000 or 4000 ppm DCM (NTP, 1986).

Based on these results, the US Environmental Protection Agency (USEPA) classified DCM as a B2 carcinogen (probable human carcinogen) and developed an oral slope factor using results in mice from NTP (1986) and Serota et al. (1986b), as well as an inhalation unit risk factor using female mouse results from the NTP study (USEPA, 1987). These values were developed using administered dose or concentration and standard defaults to extrapolate experimental findings in mice to humans.

Subsequently, a physiologically based pharmacokinetic (PBPK) model was developed for DCM by Andersen et al. (1987) to examine the importance of the known metabolic pathways, i.e., oxidative (mixed-function oxidase (MFO)) and glutathione transferase (GST) on tumor formation in laboratory animals and the potential implication in humans. Both of these pathways produce reactive intermediates that theoretically could be associated with the carcinogenic activity observed in laboratory animals. However, PBPK modeling results showed that tumor incidences from the NTP (1986) and Serota et al. (1986b) studies were consistent with calculated tissue doses from the GST pathway, which implicated a reactive glutathione metabolite, presumably *S*-(chloromethyl)glutathione, as being associated with cancer induction. (This mode of action (MOA) for DCM-associated carcinogenesis in mice has recently been reviewed (Slikker et al., 2004)). Following extensive internal and external review, the USEPA adopted the use of PBPK modeling for DCM as a reasonable means for extrapolating NTP study results in mice to humans. The unit risk factor in the USEPA Integrated Risk Information System (IRIS) for DCM was subsequently updated in 1991 to reflect PBPK modeling results—the first instance of the use of PBPK modeling by the USEPA in cancer risk assessment.

Since 1991, PBPK modeling techniques have evolved to incorporate advances in the understanding of metabolism and, in particular, statistical approaches to address variability and uncertainty. For example, probabilistic (Monte Carlo) modeling techniques have been developed that produce distributions of target tissue concentrations or internal dose metrics, rather than point estimates, and thereby reflect potential variability in input parameter values (Clewell, 1995; Thomas et al., 1996). In particular, however, Bayesian probabilistic methodology has recently been reported as a method to quantitatively address both variability and uncertainty in PBPK modeling (Gelman et al., 1996; Jonsson, 2001; Jonsson and Johanson, 2003). This methodology has also been used to address DCM (El-Masri et al., 1999; Jonsson and Johanson, 2001).

Bayesian inference offers a number of advantages in PBPK modeling, including (a) the use of experimental data and results from previous modeling efforts as starting points (priors) for model calibration; (b) the capability to update multiple variables simultaneously using a hierarchical model, rather than holding certain parameters constant, and varying others one at a time, as is undertaken using typical optimization techniques; (c) the ability to separately consider parameter variability (i.e., population heterogeneity) and uncertainty (i.e., lack of information about parameter values, which can be reduced through additional data collection) in model calibration; and (d) the capability to account for covariance of PBPK model parameters thereby precluding biased uncertainty estimates, i.e., incorrectly assuming that all variables are independent and thereby allowing related parameters to be simultaneously set at their lowest or highest values.

Although Bayesian PBPK modeling has been reported in the literature for DCM, it has been used exclusively to evaluate the influence of GST polymorphism in humans on cancer risk estimates (El-Masri et al., 1999; Jonsson and Johanson, 2001). These risk estimates were developed using probabilistic modeling for human exposure in combination with dose metrics reported in the literature for the NTP mouse study based on a deterministic mouse PBPK model. The only available Bayesian modeling of DCM in the mouse was undertaken to support the US Occupational Safety and Administration (OSHA) Final Rule on Methylene Chloride (OSHA, 1997). However, the model structure of the Andersen et al. (1987) PBPK model for DCM was modified to focus more specifically on occupational populations. Moreover, OSHA updated population distributions of physiological and partitioning parameters based on the relatively small number of mice in the available kinetic studies rather than more properly estimating these parameters from information in the general literature based on a large number of mice. Therefore, the study reported here was undertaken to apply Bayesian and dose–response modeling to the mouse in support of a new cancer risk assessment for DCM (David et al., 2005).

2. Methods

2.1. Model structure

The PBPK model structure used for this analysis is the basic structure developed by Andersen et al. (1987) (Fig. 1). The model describes the metabolism of DCM in the liver and the lung by two competing pathways: an oxidative pathway and a glutathione conjugation pathway. The cytochrome P450 (oxidative) pathway is described with saturable kinetics, whereas the glutathione transferase (GST) pathway is modeled as a first-order process.

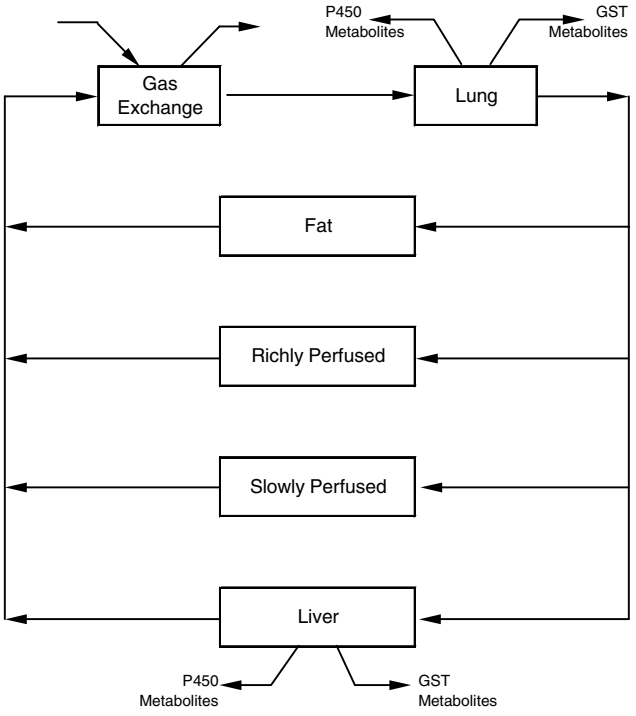

Fig. 1. Structure of the DCM PBPK model for the mouse.

For inhalation, it is assumed that chemical concentrations in inhaled air and pulmonary blood quickly achieve steady state, compared with the time required for distribution to tissues. The lung is described by two compartments: a gas exchange compartment and a metabolism compartment. This structure was assumed to allow for the equilibration of DCM between air and lung blood before it enters lung tissue (Andersen et al., 1987).

Some minor modifications were made to the model to facilitate the varying input parameter values that result from the distributional approach used in the Markov Chain Monte Carlo (MCMC) simulations. The alveolar ventilation rate was correlated with the cardiac output by replacing the parameter QPC with a ventilation/perfusion ratio (VPR), which is the ratio of alveolar ventilation rate to cardiac output. The fractional blood flows were constrained to sum to unity by dividing the fractional blood flow for each tissue by the sum of all the fractional blood flows. Likewise, the fractional tissue volumes were constrained to sum to 0.9215, which is 100% minus a constant 7.85% carcass volume, by multiplying the fractional volume of each tissue by 0.9215 and dividing by the sum of the sampled fractional tissue volumes.

2.2. Data for Bayesian analysis

Several experimental data sets, including closed-chamber inhalation experiments and intravenous injection studies, were used to calibrate the mouse model. In some of the closed-chamber experiments, the oxidative pathway was inhibited by a suicide inhibitor of cytochrome P450 2E1, *trans*-l,2-dichloroethylene (1,2-DCE), prior to exposure to DCM (Clewell et al., 1993); thus, DCM metabolism would be primarily attributed to the GST pathway. In these studies, the animals were first exposed for 1.5 h to 100 ppm *trans*-1,2-dichloroethylene, divided into groups of five, and then exposed to initial DCM concentrations of 500, 1000, or 2000 ppm. DCM uptake rates were determined by measuring the chamber DCM concentration every 5 min for the first 15 min and every 15 min thereafter (Clewell et al., 1993). Additional closed-chamber experiments were conducted with naïve animals. In this case, the closed-chamber air concentration of DCM was measured for up to 6 h in six groups ($n = 5$) of mice exposed to DCM at initial chamber concentrations of 550, 1200, 1473, 2100, 3641, or 5237 ppm in separate gas uptake experiments.

Data from intravenous (IV) injection studies were also used to calibrate the mouse model (Angelo et al., 1984). In these studies, two groups ($n = 6$) of mice were given intravenous injections of 10 and 50 mg of DCM per kg of body weight. Venous blood concentrations were measured for up to 1.5 h post injection (Andersen et al., 1987).

2.3. Markov Chain Monte Carlo analysis

Variability in pharmacokinetic parameters can be estimated from experimental data using a Bayesian optimization technique known as Markov Chain Monte Carlo (MCMC) analysis. This approach facilitates the combination of prior information about the parameter values, based on the literature and experimental data from whole animal studies, to obtain posterior distributions for the parameters (Bois, 1999, 2000; Gilks et al., 1996). It is particularly well suited for updating model parameterizations with newly available experimental data, or for recalibrating models that have been fit using less sophisticated approaches, such as visual fitting or maximum likelihood estimation for a subset of the parameters (i.e., maximizing data likelihood by varying V_{Max} and K_{M} while holding all other parameters fixed). The MCMC analysis was performed using MCSim (Bois et al., 2002), a publicly available software program for MCMC analysis (http://toxi.ineris.fr/activites/toxicologie_quantitative/mcsim/mcsim.php#article3).

For this analysis, a hierarchical population model was developed and Bayesian analysis was performed to quantify the uncertainty and variability in the PBPK model parameters for the mouse DCM model. This hierarchical population model consists of two levels—the population level and the subject or experiment level.

In the population level of the hierarchy, a distribution for the population mean ($\mathbf{M}$) of each parameter represents uncertainty about the population mean, and a distribution for the variance ($\mathbf{S}^2$) of each parameter represents uncertainty in the amount of inter-individual variability. As such, inter-individual variability is estimated separately from the uncertainty in the population mean. The population mean distribution ($\mathbf{M}$) is defined with the best estimate of the parameter mean, a standard deviation (which reflects uncertainty regarding the true population mean), and sometimes lower and upper bounds. Likewise, the population variance distribution ($\mathbf{S}^2$) is defined by a mean that reflects the best estimate of the variance of the parameter, and a standard deviation that represents uncertainty about the true amount of inter-individual variability. The population level also contains distributions for data errors ($\boldsymbol{\sigma}^2$), which are actually a combination of measurement errors and model error in the predictions of each endpoint, e.g., blood DCM concentration and closed-chamber air concentration of DCM. These combined errors were modeled using non-informative, log-uniform distributions.

In the experiment level, distributions for each subject or experimental unit were constructed by iteratively sampling mean and variance distributions for the parameters being updated, i.e., kinetic parameters, cardiac output, and the ventilation/perfusion ratio from the population level. Physiological and partitioning parameters, i.e., bodyweights, tissue blood flows, tissue volumes, and partition coefficients were not subject to updating, and these parameters were modeled more simply with one distribution that represented the experiment level mean and variability. These parameters were not subjected to updating because they are more properly estimated from information in the general literature that is based on a large number of subjects rather than being redefined based on data from the relatively small number of subjects in the kinetic studies.

The population means ($\mathbf{M}$) of the kinetic parameters were log transformed and modeled with truncated normal distributions. The population variances ($\mathbf{S}^2$) were modeled with inverse gamma distributions, as recommended by Gelman et al. (1996), with a shape parameter equal to three and an inverse scale parameter set equal to $2 \times \ln(1 + \mathrm{CV}^2)$, where the coefficient of variation (CV) was set at 50%. The inverse gamma function is defined as follows:

$$f(x;\alpha,\beta) = \frac{\beta^{\alpha}}{\Gamma(\alpha)} x^{-(\alpha-1)} \mathrm{e}^{\left(\frac{-\beta}{x}\right)},$$

where x, α, and $\beta > 0$, and where α is the shape parameter and β is the scale parameter. This parameterization corresponds to a vague prior distribution for the variance with much uncertainty (Carlin and Louis, 2000; Gelman et al., 1996).

Convergence of the Markov chains was monitored by analysis of variance as described by Gelman (1996). The estimated potential scale reduction, a ratio of an upper bound and a lower bound of the variance in the target distribution, is used to diagnose convergence. In the limit, as the number of iterations of the Markov chains goes to infinity, the ratio declines to unity. In practice, simulation of two or three independent Markov chains is continued until the estimated potential scale reduction is less than 1.2 for the means of all parameters (Gelman, 1996).

2.4. Priors

Priors were selected to reflect parameter values considered to be the most appropriate and best available. For the mouse kinetic parameters, the mean values, shown in Table 1, used to define the population mean distributions (**M**) are either the visually fitted values of Andersen et al. (1987) ($V_{Max}C$, K_M, and K_FC), or values from the OSHA final rule for occupational exposure to DCM (OSHA, 1997) (VPR, Al and A2). A default coefficient of variation (CV) of 200% was selected, with a few exceptions to avoid unnecessarily constraining the model. The CVs for VPR of 75%, and for A1 and A2 of 55% each, were based on the OSHA final rule for DCM (OSHA, 1997).

Default truncation limits were defined as the mean ± 2.5 SD rather than the mean ± 3 SD, as typically used in a Monte Carlo analysis, to facilitate convergence. However, upper truncation limits for A1 and A2 (relative lung-to-liver activities for the oxidative and conjugative metabolic pathways, respectively) were set at 1 because metabolism in the lung by either pathway is not expected to be greater than that in the liver. For the analysis of *trans*-1,2-dichloroethylene treated mice, the upper bound for $V_{Max}C$ was set to less than 2.5 SD to constrain this parameter because *trans*-1,2-dichloroethylene is a suicide inhibitor of cytochrome P450. To maintain biochemical and physiological plausibility, the lower bound for $V_{Max}C$, K_FC, A1, and A2 was set to 0.0001 for each, a lower limit of 0.01 was set for K_M, a lower bound of 10 was set for QCC, and a lower limit of 1.0 was defined for VPR because the alveolar ventilation rate would not be expected to be smaller than the cardiac output rate.

Table 2 presents distributions for the physiological parameters that were not updated in the Bayesian modeling. As noted previously, these parameters are more properly estimated from information in the general literature, which is based on a large number of mice, rather than being redefined based on data from the relatively small number of mice in the kinetic studies. The means for the blood flows and tissue volumes presented in Table 2 were set to be equal to the values in Andersen et al. (1987). The means for the partition coefficients presented in Table 2 and all CVs, with the exception of the fractional lung volume CV, were obtained from Clewell et al. (1993). The CV for the fractional lung volume was computed from the geometric standard deviation reported by OSHA (1997). Truncation limits were defined as the mean ± 2.5 SD except where biologically implausible bounds resulted (i.e., values less than 0; in which case, 0 was used).

2.5. Model calibration

Taking advantage of the Bayesian approach, the mouse calibration was divided into three sequential steps: data from closed-chamber studies with *trans*-1,2-dichloroethylene-treated mice were analyzed; followed by data from mice that were given intravenous injections of DCM, and finally data from naïve mice exposed to DCM in the closed chamber. Each step was run with three chains for a varying number of iterations to obtain convergence. The chains for the *trans*-1,2-dichloroethylene-treated mouse data were run for approximately 6000 iterations, the mouse IV data for 10,000 iterations, and naive closed-chamber mouse data for 50,000 iterations.

The approach was selected to take advantage of the different data sets. The *trans*-1,2-dichloroethylene-treated mouse data were used first because the pretreatment with *trans*-1,2-dichloroethylene essentially eliminated the oxidative metabolic pathway prior to subsequent DCM exposure. Hence, this data set permitted estimation of parameters for the glutathione conjugation pathway more precisely without interference from the competing oxidative pathway. The population mean and variance distribution definitions were updated based on the posterior distributions from this analysis. These updated distributions were then used as prior distributions to analyze the IV mouse data to estimate metabolism without the need to model pulmonary absorption processes. The population distributions were again updated based on this new set of posterior distributions, and were used as

Table 1
Prior distributions of the mouse model kinetic parameters

Parameters		**M**, population mean		**S**^{2}, Population variance			Boundary values	
		Mean	CV	Shape[f]	Inverse scale [f]	Expected CV (%)	Lower bound	Upper bound
Flow rates								
QCC[a]	Cardiac output (L/h/kg$^{0.74}$)	28	0.58	3	0.446	50	10.0	68.6
VPR[b]	Ventilation/perfusion ratio	1.52	0.75	3	0.446	50	1.0	80.1
Metabolism parameters								
$V_{Max}C_{TRANS}$[c]	Maximum metabolism rate (mg/h/kg$^{0.7}$)	0.125	2	3	0.446	50	0.0001	0.25
$V_{Max}C$[d]	Maximum metabolism rate (mg/h/kg$^{0.7}$)	11.1	2	3	0.446	50	0.0038	66.8
K_M[d]	Affinity (mg/L)	0.396	2	3	0.446	50	0.01	2.38
K_FC[d]	First-order metabolism rate (kg$^{0.3}$/h)	1.46	2	3	0.446	50	0.0001	8.76
A1[e]	Ratio of lung V_{Max} to liver V_{Max}	0.462	0.55	3	0.446	50	0.0001	1.0
A2[e]	Ratio of lung K_F to liver K_F	0.322	0.55	3	0.446	50	0.0001	1.0

[a] Population mean values are from Andersen et al. (1987). CV estimated based on OSHA (1997) to allow sufficient variability in this parameter.

[b] Population mean value calculated from OSHA (1997) (Table VI-5) geometric mean (GM) and geometric standard deviation (GSD) of 1.22 and 1.95, respectively according to following formula: population mean = $GM \times \exp((\ln(GSD)^2)/2)$. CV are from OSHA, 1997 (Table VI-7).

[c] $V_{Max}C_{TRANS}$ is the $V_{Max}C$ used for the *trans*-1,2-dichloroethylene-treated mice. CV represents a default value.

[d] Population mean values are from Andersen et al. (1987). CV represents a default value.

[e] Population mean values calculated from OSHA (1997) (Table VI-5) geometric means (GM) of 0.405 for A1 and 0.282 for A2 and geometric standard deviation (GSD) of 1.67 for each according to following formula: population mean = $GM \times \exp((\ln(GSD)^2)/2)$. CVs from OSHA (1997) (Table VI-7).

[f] The shape and inverse scale are parameters for the Inverse Gamma distribution.

Table 2
Prior distributions for the mouse model physiological parameters and partition coefficients

Parameter		Mean	CV	Lower bound	Upper bound
Fractional flow rates[a] (fraction of cardiac output)					
QFC	Fat	0.05	0.60	0	0.13
QLC	Liver	0.24	0.96	0	0.82
QRC	Rapidly perfused tissues	0.52	0.50	0	0.90
QSC	Slowly perfused tissues	0.19	0.40	0	0.38
Fractional tissue volumes[a] (fraction of body weight)					
VFC	Fat	0.04	0.30	0.01	0.07
VLC	Liver	0.04	0.06	0.034	0.046
VLuC	Lung	0.0115	0.27	0.0038	0.019
VRC	Rapidly perfused tissues	0.05	0.30	0.013	0.088
VSC	Slowly perfused tissues	0.78	0.30	0.20	0.92
Partition coefficients[b]					
PB	Blood/air	23	0.15	14	32
PF	Fat/blood	5.1	0.30	1.3	8.9
PL	Liver/blood	1.6	0.20	0.80	2.4
Plu	Lung/blood	0.46	0.27	0.15	0.77
PR	Rapidly perfused/blood	0.52	0.20	0.26	0.78
PS	Slowly perfused/blood	0.44	0.20	0.22	0.66

[a] Mean values are from Andersen et al. (1987). CVs are from Clewell et al. (1993). Boundary values = mean ± 2.5 SD unless lower bound <0, in which case 0 was used.
[b] Mean values and CVs are from Clewell et al. (1993). Boundary values = mean ± 2.5 SD.

prior distributions to analyze naïve mice exposed to DCM in the closed chamber. This latter step would include both oxidative and GST-dependent metabolism in both the lung and liver after absorption. This sequential approach was considered to more precisely calibrate metabolic parameters in the mouse model because specific aspects of DCM metabolism were addressed at each step, rather than a single overall effort to update all parameters simultaneously.

2.6. Dose–response modeling

Using the mean values from the posterior distributions, the calibrated mouse PBPK model was used to simulate inhalation exposures to DCM, following the protocol in NTP (1986). The resulting internal dose metric of mg DCM metabolized by the GST pathway/L tissue/day for both lung and liver tissue in the mouse along with tumor incidence data reported for female mice in NTP (1986), were used as input for dose–response modeling, which was consistent with USEPA (2004). Dose–response modeling was conducted with the multistage model set at two stages using the program TOX_RISK (Version 5.3). A response level of 0.1 was chosen as the point of departure, which is consistent with current USEPA practice. Internal dose metric potency factors were then calculated for lung and liver, using the point of departure and the LED_{10} (lower confidence limit of the internal dose metric associated with a 10% probability of a response in the population), i.e., $0.1/LED_{10}$. These internal dose-metric potency factors were subsequently combined with Monte Carlo analysis of the posterior distributions from the Bayesian PBPK model results in humans to develop a distribution of unit risk factors (David et al., 2005).

3. Results

3.1. MCMC analysis

The results of the sequential calibration of the mouse model are shown in Figs. 2–5 and Tables 3 and 4. Posterior distribution definitions were determined based on the last 500 lines of output for the *trans*-1,2-dichloroethylene-treated mouse data, and the IV mouse data, and on the last 2000 lines of output for the naïve closed-chamber mouse data.

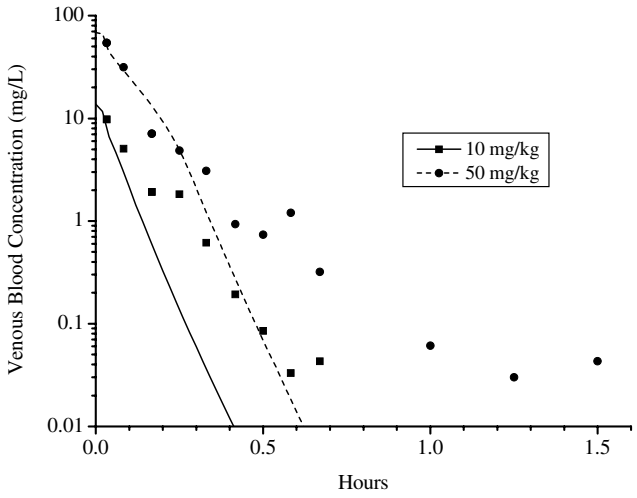

Fig. 2. IV Bayesian modeling: results using prior values.

Data were output for every fifth iteration of the chain to define the posterior distributions for each dataset. The use of longer chains was required in some cases to characterize the posterior distributions because of slow mixing in the chains. That is, the Markov chains moved very slowly across the target distribution, and it took more iterations of the chains to cover the spread of the distribution.

Scale reduction or *R*-factors were less than 1.2 for all parameters with the single exception of the *R*-factor for the blood-air partition coefficient (PB) from evaluation of the middle dose level of 1,2-DCE pretreated study animals. This *R*-factor was 1.4. However, this was the only value that exceeded 1.2 of the 283 checked, i.e., the exceedance rate was 0.35%. Moreover, *R*-factors for all remaining parameters from evaluation of the middle dose level of

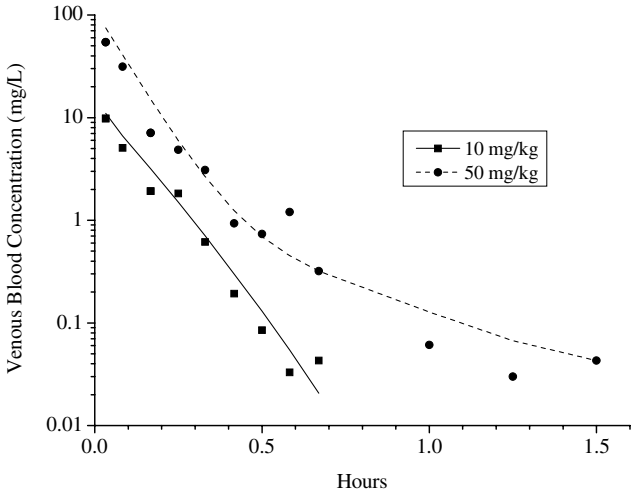

Fig. 3. IV Bayesian modeling: results using posterior values.

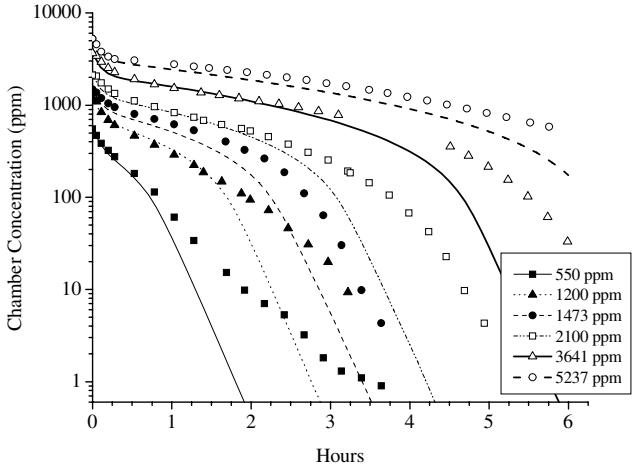

Fig. 4. Closed-chamber Bayesian modeling: results using prior values.

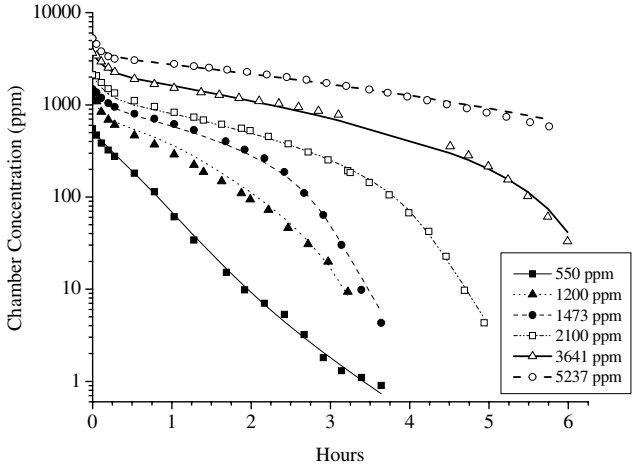

Fig. 5. Closed-chamber Bayesian modeling: results using posterior values.

1,2-DCE pretreated study animals were below 1.2 as were all *R*-factors including PB *R*-factors at both the low and high dose levels. In addition, the 1,2-DCE pretreated study dataset was the initial dataset evaluated and all *R*-factors including PB *R*-factors for all subsequent dataset evaluations were below 1.2. Finally, PB was not a parameter subject to updating. Given this information, the single incidence of an *R*-factor exceeding 1.2 is considered to have little impact on the overall results of the study.

Figs. 2 and 3 show the model fits of the IV study data using prior and posterior values, respectively. The figures show considerably improved fits using posterior values at both dose levels, i.e., 10 and 50 mg/kg. A similar result is evident regarding the closed-chamber study data. Considerably improved fits are noted in Fig. 5 (final model calibration for the mouse), using posterior values over the range of test concentrations, compared to model fits using priors, as shown in Fig. 4.

Parameter values at each stage of the sequential calibration are presented in Tables 3 and 4. Based on Michaelis–Menton enzyme kinetics, posterior mean values of $V_{\mathrm{Max}}C$ and K_{M} presented in Table 3 for the final calibration step would yield a reduced rate of oxidative metabolism of DCM in the liver for a given substrate concentration than prior values. Since priors in this case reflect values from Andersen et al. (1987), the Bayesian updating yielded a lower rate of oxidative metabolism in the liver than that reported by Andersen et al. (1987).

With the exception of A1 and A2, prior means are within one posterior standard deviation of posterior means for all parameters in Table 3. Consequently, the sequential updating produced little overall change in parameter value means. For example, little change was noted in $K_{\mathrm{F}}C$ (first-order rate constant for GST pathways), i.e., prior mean is 1.46/h, and the posterior mean of the final calibration step, i.e., closed-chamber data, is 1.41/h. Since the prior value in this case was from Andersen et al. (1987); the Bayesian updating yielded a similar activity for this pathway to that reported by Andersen et al. (1987).

Bayesian updating resulted in notable changes in values for A1 (ratio of lung to liver V_{Max}) and A2 (ratio of lung to liver K_{F}). Mean values from the posterior distribution for the final calibration step, i.e., closed-chamber data, decreased >50% for A1 and by almost 40% for A2, compared with mean values from the prior distribution, which were obtained from OSHA (1997). These results indicate that Bayesian updating yielded lower rates of metabolism in the lung, relative to the liver, for both oxidative and GST pathways, compared with OSHA (1997). Mean values from the posterior distribution of the final calibration step, i.e., closed-chamber data, were lower for Al, and higher for A2, respectively, than values reported in Andersen et al. (1987).

Table 3 also shows that the variability in all population means decreased with each sequential calibration step. For example, population mean CVs decreased from 33% for A2 (0.55–0.37) to almost an order of magnitude for $V_{\mathrm{Max}}C$ (2.0–0.21), when prior CVs are compared to final calibrated values. These results show that the calibration approach utilized in this effort resulted in considerable improvement in model precision.

Table 3
Sequential calibration of the mouse model kinetic parameter means (**M**)

Parameter		Prior distributions		Posterior distributions					
				TRANS treated[a]		IV injection		Closed-chamber	
		Mean	CV	Mean	CV	Mean	CV	Mean	CV
Flow rates									
QCC	Cardiac output (L/h/kg$^{0.74}$)	28.0	0.58	24.2	0.19	—	—	—	—
VPR	Ventilation/perfusion ratio	1.52	0.75	1.45	0.20	—	—	—	—
Metabolism parameters									
$V_{Max}C_{TRANS}$[b]	Maximum metabolism rate (mg/h/kg$^{0.7}$)	0.125	2	0.0767	1.6	—	—	—	—
$V_{Max}C$	Maximum metabolism rate (mg/h/kg$^{0.7}$)	11.1	2	—	—	2.12	1.0	9.27	0.21
K_M	Affinity (mg/L)	0.396	2	—	—	0.395	0.85	0.574	0.42
K_FC	First-order metabolism rate (kg$^{0.3}$/h)	1.46	2	1.30	0.30	1.29	0.30	1.41	0.28
A1	Ratio of lung V_{Max} to liver V_{Max}	0.462	0.55	0.325	0.42	0.275	0.39	0.207	0.36
A2	Ratio of lung K_F to liver K_F	0.322	0.55	0.264	0.46	0.233	0.41	0.196	0.37

[a] TRANS treated refers to the *trans*-1,2-dichloroethylene-treated mice.
[b] $V_{Max}C_{TRANS}$ is the $V_{Max}C$ used for the *trans*-1,2-dichloroethylene-treated mice.

Table 4
Sequential calibration of the mouse model kinetic parameter variances (**S**^{2})

Parameter	Prior distributions				Posterior distributions											
					TRANS-pretreated				IV injection				Closed-chamber			
	CV[a]	CU[b]	Shape	Inverse scale	CV[a]	CU[b]	Shape	Inverse scale	CV[a]	CU[b]	Shape	Inverse scale	CV[a]	CU[b]	Shape	Inverse scale
Flow rates																
QCC	0.5	1	3	392	0.43	0.55	5.3	462	—	—	—	—	—	—	—	—
VPR	0.5	1	3	0.45	0.39	0.62	4.6	0.52	—	—	—	—	—	—	—	—
Metabolism parameters																
$V_{Max}C$	0.5	1	3	0.45	—	—	—	—	0.58	1.2	2.7	0.48	0.43	0.67	4.2	0.55
K_M	0.5	1	3	0.45	—	—	—	—	0.5	0.81	3.5	0.57	0.48	0.64	4.4	0.7
K_FC	0.5	1	3	0.45	0.46	0.63	4.5	0.66	0.48	0.8	3.6	0.53	0.47	0.64	4.4	0.68
A1	0.5	1	3	0.45	0.49	0.68	4.2	0.68	0.48	0.59	4.9	0.8	0.48	0.53	5.5	0.93
A2	0.5	1	3	0.45	0.49	0.76	3.7	0.59	0.5	0.66	4.3	0.74	0.5	0.56	5.2	0.93

QCC, cardiac output (L/h/kg$^{0.74}$); VPR, ventilation/perfusion ratio; $V_{Max}C$, maximum metabolism rate (mg/h/kg$^{0.7}$); K_M, affinity (mg/L); K_FC, first-order metabolism rate (kg$^{0.3}$/h); A1, ratio of lung V_{Max} to liver V_{Max}; A2, ratio of lung K_F to liver K_F.
[a] Coefficient of variation at the mean of the population distributions. These values were calculated as follows: $CV = \frac{\sqrt{\text{sample mean of variance distribution}}}{\text{sample mean of the mean distribution}}$ (QCC, which was not log transformed); $CV = \sqrt{e^{(\text{sample mean of variance distribution})} - 1.0}$ (All other parameters, as these were log-transformed).
[b] Coefficient of uncertainty in the variance distribution. This value was calculated as follows: $CU = \frac{\text{sample standard deviation of the variance distribution}}{\text{sample mean of the variance distribution}}$.

The variance distributions are more difficult to interpret, hence, these results are presented in Table 4 in terms of coefficients of variation (CV) and uncertainty (CU) for illustration, as well as inverse gamma shape and scale. The values are estimated from the sample means and sample standard deviations computed from the posterior distributions. The CV values presented in Table 4 are the mean CVs, i.e., the coefficient of variation at the mean of the population distributions. These values reflect the mean of the final population variance distribution (**S**^{2}) divided by the mean of the final population mean distribution (**M**). For each parameter in Table 4, these CVs changed very little across the three different steps suggesting that inter-individual variability was relatively unaffected by model calibration. The CU values presented in Table 4 are the coefficients of uncertainty in the variance distribution, i.e., the standard deviation of the final population variance (**S**^{2}) distribution divided by mean of the final population variance (**S**^{2}) distribution. These CUs tended to decrease across the various data sets, and because the population variance distribution (**S**^{2}) reflects uncertainty regarding inter-individual variation, these results suggest that model calibration tended to reduce the uncertainty in inter-individual variability for all updated parameters.

3.2. Dose–response modeling

Using the mean values from the posterior distributions, the calibrated mouse PPBK model was used to simulate exposures to DCM following the protocol in NTP (1986), i.e., five daily inhalation exposures of 6 h each followed by two non-exposure days/week. The simulation was run until periodicity was reached, i.e., no change in internal dose metrics was noted (18 weeks), and the average daily amount of DCM metabolized by the GST pathway (mg DCM/L tissue/day) was determined from the last seven simulation days. A bodyweight of 34.5 g was used, which

reflects the weighted average of group mean terminal bodyweights from NTP (1986), and is consistent with the bodyweight used in the Andersen et al. (1987) and USEPA (1987) PBPK models.

The resulting internal dose metrics for both lung and liver tissue of average daily mg DCM metabolized by the GST pathway/L tissue/day and tumorigenicity incidence data from NTP (1986) were used as inputs for dose–response modeling with the program TOX_RISK (Version 5.3). Consistent with current USEPA methodology, the multistage model was run with two stages, and a point of departure for the dose–response modeling of 10% extra risk. The LED_{10}s were 39.12 mg/L tissue/day (ED_{10} of 53.56 mg/L tissue/day) based on the incidence of the lung adenomas and carcinomas, and 642.56 mg/L tissue/day (ED_{10} of 1170.3 mg/L tissue/day) based on the incidence of liver adenomas and carcinomas. These values yielded internal dose metric potency factors, i.e., $0.1/LED_{10}$, of 2.56×10^{-3}/(mg/L tissue/day) for the lung, and 1.56×10^{-4}/(mg/L tissue/day) for the liver. These internal dose-metric potency factors were subsequently combined with Bayesian PBPK modeling results in humans that included data on GST polymorphisms to derive a distribution of unit risk factors (David et al., 2005).

Table 5 presents the lung and liver dose metrics used in the dose–response modeling, along with those reported by Andersen et al. (1987) and USEPA (1987). Differences of approximately 3- to 4-fold are attributable mainly to the use of improved partition coefficients (Clewell et al., 1993), as well as refined kinetic parameters resulting from Bayesian updating. This difference in internal dose metrics translated to a comparable difference in LED_{10}s and internal dose metric potency factors.

Table 5
Dose–response modeling information

Target organ	NTP exposure level	Number of animals with tumor[a]	Number of animals	Dose metrics[b]			Potency factors[c]		
				Bayesian model	Andersen et al. (1987)	USEPA (1987)	Bayesian model[d]	Andersen et al. (1987)[e]	USEPA (1987)[f]
Liver	Control	3	45	0	0	0			
	2000 ppm	16	46	2359.99	851	727.8	1.56E−04	4.42E−04	5.59E−04
	4000 ppm	40	46	4869.85	1811	1670			
Lung	Control	3	45	0	0	0			
	2000 ppm	30	46	474.991	123	111.4	2.56E−03	9.80E−03	1.06E−02
	4000 ppm	41	46	973.343	256	243.7			

[a] Number of animals with either a carcinoma, adenoma or both.
[b] mg DCM metabolized by GST pathway/L tissue/day.
[c] Potency factor (mg DCM metabolized by (GST pathway/L tissue/day)$^{-1}$) = $0.1/LED_{10}$.
[d] LED_{10}s using the multistage model were 39.12 and 642.56 mg/L/day for lung and liver, respectively.
[e] LED_{10}s using the multistage model were 10.2 and 226.3 mg/L/day for lung and liver, respectively.
[f] USEPA used a different breathing rate (0.043 m^3/d) in its PBPK modeling to derive dose metrics rather than to the Andersen et al. (1987); breathing rate (0.084 m^3/d). Cardiac output was set equal to alveolar ventilation. LED_{10}s for USEPA dose metrics using the multistage model were 9.46 and 178.9 mg/L/day for lung and liver, respectively.

4. Discussion

This report presents the results of Bayesian PBPK and dose–response modeling of DCM in mice. A hierarchical model was developed consistent with approaches reported by other investigators (Bernillon and Bois, 2000; Jonsson, 2001). For this effort, kinetic model parameters ($V_{Max}C$, K_M, K_FC, A1, and A2) were updated in a sequential manner with experimental results from studies in mice, whereas other model parameters (bodyweight, partition coefficients, and tissue blood flows) were not. As noted previously, these latter parameters are more properly estimated from information in the general literature that is based on a large number of mice rather than being redefined based on data from the relatively small number of mice in the kinetic studies. The sequential updating was designed to calibrate the model in stages, i.e., closed-chamber study results in mice treated with *trans*-1,2-dichloroethylene, a suicide inhibitor of cytochrome P450 2E1, were used first to estimate K_FC (GST pathway), IV study data in mice were then used to estimate the contribution of the cytochrome P450 pathway without introducing potential variability of absorption and excretion processes in the lung during inha-

lation, and finally, closed-chamber study data were used to incorporate these later processes. This approach resulted in an improved calibration procedure than would have resulted from analyzing all data sets simultaneously. Results show that each calibration step reduced model uncertainty and produced good fits to the modeled datasets. This is the first reported effort undertaken with this approach for DCM in mice.

This effort differs from that of OSHA (1997) in a number of important aspects. The OSHA Bayesian modeling effort included updating physiological and partitioning parameter distributions, and, as such, parameter values that are best determined by literature references or larger studies were estimated by OSHA with study results from small experiments. Moreover, sequential calibration of the mouse model did not include IV studies to estimate cytochrome P450-dependent metabolism activity, apart from confounding processes of absorption and excretion of DCM from the lung during inhalation. Normalization of blood flows and tissue volumes was undertaken by adjusting values for a single compartment to account for incidences where random selection produced blood flows to tissues that exceeded cardiac output, or total tissue volumes that exceeded bodyweight. (Blood flows and tissue volumes in this study were proportionally adjusted to ensure that total flows and volumes did not exceed cardiac output or bodyweight, consistent with more typical approaches for PBPK modeling (Clewell, 1995; Gelman et al., 1996)). Finally, the OSHA PBPK model reflects a modified model structure that was designed to address occupational populations compared with that of Andersen et al. (1987).

The PBPK model structure for the mouse used in this effort is that of Andersen et al. (1987). Recently, Sweeney et al. (2004) reported better fits to certain human time course exposure profiles if extrahepatic metabolism (10% of liver cytochrome P450-dependent metabolism added to the slowly perfused tissue compartment) was included in the PBPK model. This study involved exposure to low DCM concentrations. Extrahepatic metabolism was not added to the mouse PBPK model for a number of reasons. Fig. 6 presents the percent difference in the amount of DCM metabolized/L tissue/day by the oxidative and GST pathways in the lung and liver of mice with and without extrahepatic metabolism at exposure concentrations of 50, 100, 250, 500, 1000, 2000, or 4000 ppm. Consistent with Sweeney et al. (2004), extrahepatic metabolism, i.e., 10% of the liver rate of oxidative metabolism was included in the slowly perfused tissue compartment. As shown in Fig. 6, PBPK model results using the Andersen et al. (1987) PBPK model showed that extrahepatic metabolism was more important at lower concentrations with negligible effect on metabolite production in the lung or liver at higher concentrations. For example, there was a 5–6% reduction in formation of GST metabolites in the lung and liver at 50 ppm if extrahepatic metabolism was included in PBPK modeling. In

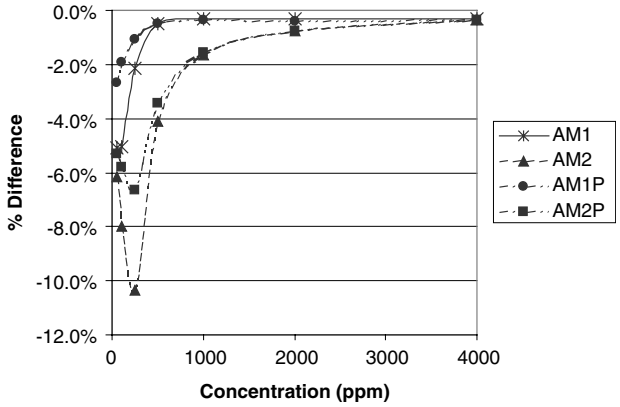

Fig. 6. Percent difference in the amount of DCM metabolized by MFO and GST pathways with and without extrahepatic metabolism. AM1, Amount DCM metabolized by MFO pathway in liver/L tissue/day; AM2, Amount DCM metabolized by GST pathway in liver/L tissue/day; AM1P, Amount DCM metabolized by MFO pathway in lung/L tissue/day; AM2P, Amount DCM metabolized by GST pathway in lung/L tissue/day.

contrast, there was only a 0.77 or 0.37% reduction, respectively at 2000 and 4000 ppm, the two concentrations used in the NTP (1986) bioassay. As such, inclusion or exclusion of extrahepatic metabolism in the mouse model was judged as having little potential effect on resultant dose metrics or dose–response modeling results. Moreover, closed-chamber mouse studies used for Bayesian-model calibration in the present effort involved exposure concentrations of 550–5237 ppm, levels for which extrahepatic metabolism would have negligible impact on model calibration. Finally, the PBPK modeling results in the mouse presented in Fig. 6 were consistent with Bayesian modeling of various human data sets, which showed that extrahepatic metabolism was reduced in studies using higher exposure concentrations (David et al., 2005).

Using treatment levels from the NTP (1986) mouse bioassay, the calibrated PBPK model yielded internal dose metrics for the mouse that were increased by 3- to 4-fold, compared with those reported by Andersen et al. (1987) or the USEPA (1987). This difference is mainly attributable to the use of improved partition coefficients (Clewell et al., 1993), as well as refined kinetic parameters resulting from Bayesian updating. As noted previously, Bayesian modeling is well suited for updating model parameterizations with newly available experimental data, or for recalibrating models that have been fit using less sophisticated approaches, such as visual fitting or maximum likelihood estimation for a subset of the parameters (i.e., maximizing data likelihood by varying V_{Max} and K_M while holding all other parameters fixed).

Deterministic dose–response modeling was undertaken for this study, consistent with current USEPA methodologies. This approach is also consistent with that reported by Jonsson and Johanson (2001). Although probabilistic approaches have been reported, such approaches have inherent methodological difficulties. Probabilistic approaches

would typically involve randomly selecting points from each dose metric distribution.

For a subset of these selections, however, dose–response modeling would not yield acceptable fits, e.g., a dose metric from the higher exposure group is either equal to, or lower than, the selected dose metric from the lower exposure group. Typically, model results yielding poor fits are rejected, and in this case, doing so would eliminate validly selected dose metrics from the output distribution of ED_{10}s or LED_{10}s. OSHA (1997) alleviated potentially poorly fitting dose–response curves by apparently using the same physiological parameter values to generate dose metrics at different exposure levels. However, this approach also does not account for the full range of potential outcomes from dose–response modeling. Because of these difficulties with probabilistic dose–response modeling and to be consistent with current USEPA methodology, a deterministic approach was selected, and both ED_{10}s and LED_{10}s were generated for potential use in developing unit risk factors. The LED_{10} or the lower bound of the ED_{10} reflects a statistical adjustment so that there would only be a 5% chance or less that the "true" maximum likelihood estimate could be lower, and therefore, it would address, in part, variability in modeling or experimental datasets. LED_{10}s in the lung and liver from this effort were used to generate internal dose metric potency factors, i.e., $0.1/LED_{10}$, and subsequently combined with Bayesian PBPK model results in humans that included GST polymorphism to derive an inhalation unit risk factor for DCM. This subsequent effort is reported in David et al. (2005).

5. Conclusion

Bayesian PBPK and dose–response modeling were undertaken in the mouse for DCM and the results show that internal dose metrics from the calibrated mouse model are 3- to 4-fold higher than values used by USEPA to derive its current unit risk factor for DCM. This difference is mainly attributable to the use of improved partition coefficients (Clewell et al., 1993), as well as refined kinetic parameters resulting from Bayesian updating. Bayesian modeling is known to be particularly well suited for updating model parameterizations with newly available experimental data, or for recalibrating models that have been fit using less sophisticated approaches, such as visual fitting or maximum likelihood estimation for a subset of the parameters. Therefore, the results of this effort are particularly well suited for derivation of an improved unit risk factor for DCM (David et al., 2005).

Acknowledgments

The authors express their appreciation to Dr. Thomas Starr and Dr. M.W. Anders for their insightful suggestions and thoughts regarding the design and conduct of this effort and regarding the preparation of the manuscript.

References

Ahmed, A.E., Anders, M.W., 1978. Metabolism of dihalomethanes to formaldehyde and inorganic halide. I. In vitro studies. Drug Metab. Dispos. 4, 357–361.

Andersen, M.E., Clewell, H.J., Gargas, M.L., Smith, F.A., Reitz, R.H., 1987. Physiologically based pharmacokinetics and the risk assessment for methylene chloride. Toxicol. Appl. Pharmacol. 87, 185–205.

Angelo, M.J., Bischoff, K.B., Pritchard, A.B., Presser, M.A., 1984. A physiological model for the pharmacokinetics of methylene chloride in B6C3F1 mice following i.v. administration. J. Pharmacokinet. Biopharm. 12, 413–436.

Bernillon, P., Bois, F.Y., 2000. Statistical issues in toxicokinetic modeling: A Bayesian perspective. Environ. Health Perspect. 108 (5), 883–893.

Bois, F., 1999. Analysis of PBPK models for risk characterization. Ann. N. Y. Acad. Sci. 895, 317–337.

Bois, F., 2000. Statistical analysis of Clewell et al. PBPK model of trichloroethylene kinetics. Environ. Health Perspect. 108 (2), 307–316.

Bois, F., Maszle, D., Revzan, K., Tillier, S., Yuan, Z., 2002. MCSim Version 5 beta 2. <http://toxi.ineris.fr/activites/toxicologie_quantitative/mcsim/article3/>.

Burek, J., Nitschke, K., Bell, T., Wackerle, D., Childs, R., Beyer, J., Dittenber, D., Rampy, L., McKenna, M., 1984. Methylene chloride: a two-year inhalation toxicity and oncogenicity study in rats and hamsters. Fundam. Appl. Toxicol. 4, 30–47.

Carlin, B.P., Louis, T.A., 2000. Bayes and Empirical Bayes Methods for Data Analysis, second ed. CRC Press LLC, Boca Raton.

Clewell, H.J., Gearhart, J.M., Andersen, M.E., 1993. analysis of the metabolism of methylene chloride in the B6C3F1 mouse and its implications for human carcinogenic risk. Submission to OSHA Docket #H-071, Exhibit #96.

Clewell, H.J., 1995. The use of physiologically based pharmacokinetic modeling in risk assessment: a case study with methylene chloride. In: Olin, S., Farland, W., Park, C., Rhomberg, L., Scheuplein, R., Starr, T., Wilson, J. (Eds.), Low-Dose Extrapolation of Cancer Risks: Issues and Perspectives. ILSI Press, Washington, DC, pp. 199–221.

David, R.M., Clewell, H.J., Gentry, P.R., Covington, T., Morgott, D.A., Marino, D.J., 2005. Revised assessment of cancer risk to cichloromethane using improved human metabolic parameters and bayesian statistics. Reg. Pharmacol. Toxicol Submitted.

El-Masri, H.A., Bell, D.A., Portier, C.J., 1999. Effects of glutathione transferase theta polymorphism on the risk estimates of dichloromethane to humans. Toxicol. Appl. Pharmacol. 158, 221–230.

Gelman, A., 1996. Inference and monitoring convergence. In: Gilks, W.R., Richardson, S., Spiegelhalter, D.J. (Eds.), Markov Chain Monte Carlo in Practice. Chapman and Hall/CRC, Boca Raton, FL, pp. 131–143.

Gelman, A., Bois, F., Jiang, J., 1996. Physiological pharmacokinetic analysis using population modeling and informative prior distributions. J. Am. Stat. Assoc. 91 (436), 1400–1412.

Gilks, W.R., Richardson, S., Spiegelhalter, D.J., 1996. Markov Chain Monte Carlo in Practice. Chapman and Hall/CRC, Boca Raton, FL.

Holbrook, M.T., 1993. Methylene chloride, fourth ed.. In: Kroschwitz, J.I. (Ed.), Kirk-Othmer Encyclopedia of Chemical Technology, vol. 5 John Wiley, New York, NY, pp. 1041–1050.

Jonsson, F., 2001. Physiologically based pharmacokinetic modeling in risk assessment: development of Bayesian population methods. National Institute for Working Life. Stockholm, Sweden. <http://www.diva-portal.org/diva/getDocument?urn_nbn_se_uu_diva-257-1_fulltext.pdf/>.

Jonsson, F., Johanson, G., 2001. A Bayesian analysis of the influence of GSTT1 polymorphism on the cancer risk estimate for dichloromethane. Toxicol. Appl. Pharmacol. 174, 99–112.

Jonsson, F., Johanson, G., 2003. The Bayesian population approach to physiological toxicokinetic–toxicodynamic models—an example using the MCSim software. Toxicol. Lett. 138 (8), 143–150.

National Coffee Association, 1982. Twenty-four month chronic toxicity and oncogenicity study of methylene chloride in rats. Unpublished

report, Hazleton Laboratories America, Inc., Vienna VA, as cited in NTP (1986).

National Coffee Association, 1983. Twenty-four month chronic toxicity and oncogenicity study of methylene chloride in mice. Final report, Hazleton Laboratories America, Inc., Vienna VA, as cited in NTP (1986).

National Toxicology Program (NTP), 1986. Toxicology and carcinogenesis studies of dichloromethane (methylene chloride) (CAS No. 75-09-2) in F344/N rats and B6C3F1 mice (inhalation studies). NTP-TR-306.

Nitschke, K.D., Burek, J.D., Bell, TJ., Kociba, R.J., Rampy, L.W., McKenna, M.J., 1988. Methylene chloride: a 2-year inhalation toxicity and oncogenicity study in rats. Fundam. Appl. Toxicol. 11, 48–59.

Occupational Safety and Health Administration (OSHA), 1997. Occupational Exposure to Methylene Chloride. Fed. Reg. vol. 62, No. 7, pp 1493–1619.

Serota, D.G., Thakur, A.K., Ulland, B.M., Kirschman, J.C., Brown, N.M., Coots, R.H., Morgareidge, K., 1986a. A two-year drinking water study of dichloromethane in rodents. I. Rats. Food Chem. Toxicol. 24, 951–958.

Serota, D.G., Thakur, A.K., Ulland, B.M., Kirschman, J.C., Brown, N.M., Coots, R.H., Morgareidge, K., 1986b. A two-year drinking water study of dichloromethane in rodents. I. Mice. Food Chem. Toxicol. 24, 959.

Slikker Jr., W., Andersen, M.E., Bogdanffy, M.S., Bus, J.S., Cohen, S.D., Conolly, R.B., David, R.M., Doerrer, N.G., Dorman, D.C, Gaylor, D.W., Hattis, D., Rogers, J.M., Setzer, R.W., Swenberg, J.A., Wallace, K., 2004. Dose-dependent transitions in mechanisms of toxicity: case studies. Toxicol. Appl. Pharmacol. 201 (3), 226–294.

Sweeney, L.M., Kirman, C.R., Morgott, D.A., Gargas, M.L., 2004. Development of a refined physiologically based pharmacokinetic model for dichloromethane and application to estimation of interindividual variation in oxidative metabolism in human volunteers. Toxicol. Lett. 154, 201–216.

Thomas, R.S., Lytle, W.E., Keefe, T.J., Constan, A.A., Yang, R.S., 1996. Incorporating Monte Carlo simulation into physiologically based pharmacokinetic models using advanced continuous simulation language (ACSL): a computational method. Fundam. Appl. Toxicol. 31 (1), 19–28.

United States Environmental Protection Agency (USEPA), 1987. Technical Analysis of New Methods and Data Regarding Dichloromethane Hazard Assessments Office of Health and Environmental Assessment. EPA/600/8-87/029A. June 1987.

United States Environmental Protection Agency (USEPA), 2004. Integrated Risk Information System: Dichloromethane. <www.epa.gov/iris/subst/0070.htm/>.